DOI 10.36146/2026_0708_13

La Metallurgia Italiana
International Journal of the Italian Association for Metallurgy

Effect of hydrogen oxyfuel combustion on oxide scale descalability by thermal shock for low-carbon steels

S. Airaksinen, K. Siltala, J. Haapakangas, A. Heikkilä, Q. Shu

Steel industry is in transition concerning heating methods due to requirement to reduce CO_2 emissions. Use of hydrogen as a fuel in combustion for heating makes the reheating furnace a possible method to reduce use of fossil fuels, and oxyfuel combustion increases efficiency of the heating process compared to air-fuel method. Oxide scale formation of two low carbon steels is studied under isothermal tests at 1200 °C for 2 hours with methane-air, methane-oxygen, and hydrogen-oxygen combustion atmospheres using free oxygen contents of 1% and 6%. Both steels contained silicon, but Steel A had higher amounts of manganese and Steel B had higher amounts of chromium and nickel. Descaling efficiency of oxidized samples is studied by thermal shock. Characterization for oxidized and descaled cross-sections of samples was performed by digital microscopy and field-emission scanning electron microscopy (FESEM). Results show that more nickel and chromium containing Steel B produces less oxide scale in all studied atmospheres, but its descaling efficiency by thermal shock is weaker compared to Steel A. Descaling efficiency decreases for both steels by changing heating method from methane-air to hydrogen-oxygen. Decrease of free oxygen content removes oxide scale from wider surface area. Steel B has more entanglement structure with deeper scale penetrations at oxide-steel interface, making its adherence higher. Thickness of interface scale for both steels after thermal shock decreases from methane-air method to hydrogen-oxygen method.

KEYWORDS: HYDROGEN COMBUSTION; OXYFUEL; REHEATING; LOW-CARBON STEEL; OXIDE SCALE; DESCALING.

INTRODUCTION

Hydrogen fuel combustion provides CO_2-free heating methods for reheating furnaces compared to natural gas combustion, and efficiency of heating methods can be increased by changing combustion from air-fuel to oxyfuel. The complete combustion of the fuel gas is ensured by excess oxidant, providing free oxygen in the furnace gas atmosphere. Free oxygen content is kept low in industrial reheating furnace, typically around 2-5% [1-2], to prevent material loss due to excessive oxidation. Transition from natural gas combustion with air to hydrogen combustion with oxygen increases proportion of water vapor in furnace gas atmosphere. Oxidizing atmosphere produces oxide scale on the steel surface, and higher water vapor content has an increasing effect on the oxide scale formation [3].

After reheating, oxide scale is removed by hydraulic descaling to provide cleaner surface for hot rolling process.

Susanna Airaksinen, Konsta Siltala, Juho Haapakangas, Anne Heikkilä, Qifeng Shu
Process metallurgy, University of Oulu, Finland

Hydraulic descaling is based on thermal shock by water for hot surface of steel and mechanical impact by high pressure jets with descaling parameters such as pressure, working distance, and lead angle [4]. Thermal shock has wider impact area compared to mechanical impact, and it is observed to be the main method for descaling [5, 6]. Efficiency of thermal shock is based on different thermal expansion coefficients of steel and oxide scale, which cause cracking on oxide scale and peeling of it from the steel surface [5].

Steel elemental composition and heating conditions (temperature, time, atmosphere) were observed to affect the descaling. Increasing silicon and nickel contents develop entanglement structure of oxide-steel interface, decreasing descaling efficiency.[1] Free oxygen content in furnace gas atmosphere has found to have the most significant difference on thickness of residual oxide scale on the steel surface using 1150 °C temperature [7]. Increase of water vapor content from 18 to 32% based on air-combustion change from natural gas to hydrogen is not observed to affect oxide scale removability by water jets [8].

In this study, oxides gas combustion of low-carbon steels was studied under isothermal tests at 1200 °C for 2 hours using simulated combustion gas atmospheres with 1% and 6% free oxygen. The aim of the work was to investigate how the change of combustion method from natural gas to hydrogen and air-fuel to oxyfuel affects oxide scale descalability using water thermal shock.

MATERIALS AND METHODS

Two different low-carbon steel grades were supplied by Ovako Imatra Oy Ab. Composition of steel grades are presented in table 1. The sample size was 12 mm × 12 mm × 30 mm, and the actual dimensions of each sample were measured using average of three measurements for the determination of surface area. A diameter of 2 mm hanging hole was drilled on the top of each sample. Before heating tests, the samples were polished with SiC 220 grit paper, cleaned with ethanol, and dried using temperature of 105 °C.

Tab.1 - Composition of low-carbon steels (wt.%).

STEEL COMPOSITION										
Steel	C	Si	Mn	P	S	Cr	Ni	Mo	Cu	Al
A	0.15	0.22	1.16	0.01	0.03	0.17	0.13	0.03	0.21	0.02
B	0.14	0.29	0.55	0.01	0.01	1.62	1.51	0.26	0.20	0.03

Heating tests were performed in a vertical tube furnace, producing thermogravimetry (TG) data by hanging sample inside the furnace from the digital scale. Time of isothermal heating at 1200 °C was 2 hours. The sample was placed inside the furnace with 100% nitrogen atmosphere to prevent oxidation during pre-heating for 10 minutes before test. After test, the sample was removed from the furnace and placed in the cooling box with argon gas flow or dipped in the water vessel for faster cooling.

Heating atmospheres simulate the combustion of natural gas or hydrogen with air or oxygen as oxidant. The main component of natural gas is methane (CH_4), which is used as fuel gas in calculations for heating atmosphere composition after combustion. Studied atmospheres were methane-air (MA), methane-oxygen (MO), and hydrogen-oxygen (HO). Different shares of excess oxidant were used in calculations to provide suitable free oxygen content to the heating atmosphere. Gas composition of each heating atmosphere is presented in table 2. During test, the gas mixture of heating atmosphere was fed to the furnace at 2 L min^{-1}.

After heating tests, the samples were cold mounted in epoxy, cut in half, and polished for cross-section characterization. Digital microscope was used for characterization

of oxide scale structure and measurement of structural lengths. Average thickness of oxide scale at oxide-steel interface after thermal shock was measured from the three points at center area of each sample side (12 points in total). Average penetration depth of oxide scale into the steel matrix was measured from all penetrations on one sample side. FESEM (Zeiss Ultra plus) equipped with EDS was used for analysis of oxide scale structure with chemical composition. FESEM imaging was performed using backscattered electrons (BSE).

Tab.2 - Gas composition of heating atmospheres (vol.%).

GAS COMPOSITION				
Atmosphere ID	CO_2	H_2O	N_2	O_2
MA1	9.1	18.1	71.8	1.0
MA6	6.8	13.6	73.6	6.0
MO1	33.0	66.0	-	1.0
MO6	31.3	62.6	-	6.0
HO1	-	99.0	-	1.0
HO6	-	94.0	-	6.0

RESULTS AND DISCUSSION

Differences in oxide scale formation

Total weight gain results of samples are presented in table 3 and weight gain with respect to time is presented in figure 1. The results show that higher free oxygen content (6% O_2) in furnace atmosphere produced more oxide scale compared to lower oxygen content (1% O_2) for both steel grades, as expected based on literature [7, 9-10]. Effect of free oxygen content was greater for methane-air (MA) method than hydrogen-oxygen (HO) method, when the increase of weight gain was 56% between MA methods and about 20% between HO methods. Correspondingly, a greater effect of free O_2 in heating atmosphere on oxide scale formation has also been observed in dynamic heating for MA method compared to HO method, when oxygen content changed from 1% to 2.5% [10]. Difference between free oxygen contents is lower for HO method due to having significantly higher water vapor content. Water vapor promotes internal oxidation of iron by inward transport and dissociation of H_2O, producing oxygen inside the oxide scale [11]. Thus, at high water vapor contents in gas atmosphere, the effect of H_2O produced oxygen increases, decreasing the difference between HO1 and HO6 methods.

Increase of water vapor content in furnace gas atmosphere, when the fuel gas is changed from methane to hydrogen and oxygen is used as oxidant compared to air, increased oxidation for both steels. In comparison between MA6 and HO6 atmospheres, oxide scale formation increased by 55% for Steel A and 41% for Steel B. Heating methods with higher free oxygen content have the lower proportions of water vapor and carbon dioxide in atmosphere. However, based on the oxidation results that higher O_2 content produces more oxide scale, the decrease in H_2O and CO_2 content was not as significant as amount of free oxygen in these heating conditions.

Amount of oxide scale was higher for Steel A compared to Steel B using all studied atmospheres, which was attributed to the lower Ni and Cr amounts of Steel A. The higher Ni content of Steel B presumably reduced the oxidation rate due to the slow diffusion of nickel in iron, causing nickel enrichment at oxide-steel interface. Diffusivity of iron and oxygen is lower in nickel than in iron, reducing oxide scale formation. [12] Furthermore, higher chromium alloying can form $FeCr_2O_4$, which acts as a diffusion barrier for ions, decreasing the oxidation rate [13]. Steel A has higher Mn content than Steel B, which can decrease the oxidation rate with high manganese content at 650 °C

[14]. However, Fe-Mn alloys with low manganese contents (1-5 wt-%) were not detected significant difference in oxidation rates at 1150 °C for 20 minutes [15]. In this study, the effect of Mn on oxide scale formation remained low in relation to chromium and nickel.

Tab.3 - Total weight gain of samples after heating test (mg/cm²)

TOTAL WEIGHT GAIN						
Steel	MA1	MA6	MO1	MO6	HO1	HO6
A	114.6	178.3	214.3	264.6	224.3	276.5
B	113.2	176.7	191.7	246.0	212.0	248.9

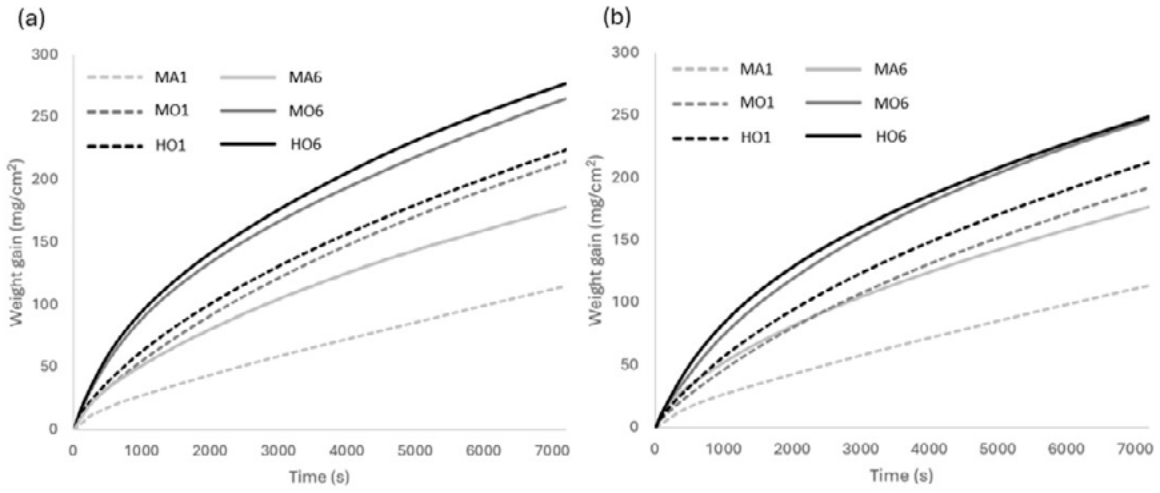

Fig.1 - Weight gain during heating tests: a) Steel A and b) Steel B.

Oxide scale structures using different furnace atmospheres for both steel grades are presented in figure 2. Low O_2 produced sharp-shaped surface on the oxide-gas interface, while the surfaces of high O_2 samples were smooth. Due to low O_2 levels, iron oxide formed is mainly wüstite (FeO), because it requires lower partial pressure compared to magnetite (Fe_3O_4) and hematite (Fe_2O_3), but magnetite precipitates is found inside and above wüstite layer. Using higher O_2 content (6%), magnetite layer and a thin hematite layer formed above the wüstite layer as seen in figure 3 and table 4. Similar observations from outer iron oxide phases are presented in previous studies [10,16].

Shape of pores inside the oxide scale was different between atmospheres, because the shape was more horizontally layered for MA atmospheres and round-shaped for oxyfuel atmospheres (MO, HO). Difference of pore shapes is discussed in previous study [17]. Furthermore, Steel B exhibited visually higher porosity and a greater number of pores than Steel A in the MO and HO atmospheres, which may be attributed to differences in alloying between the steel grades. For example, nickel is presented to increase oxide scale porosity. Due to difference in diffusion rates of iron and nickel, outward diffusion of iron generates and condensates vacancies at oxide-steel interface, forming voids [12, 18].

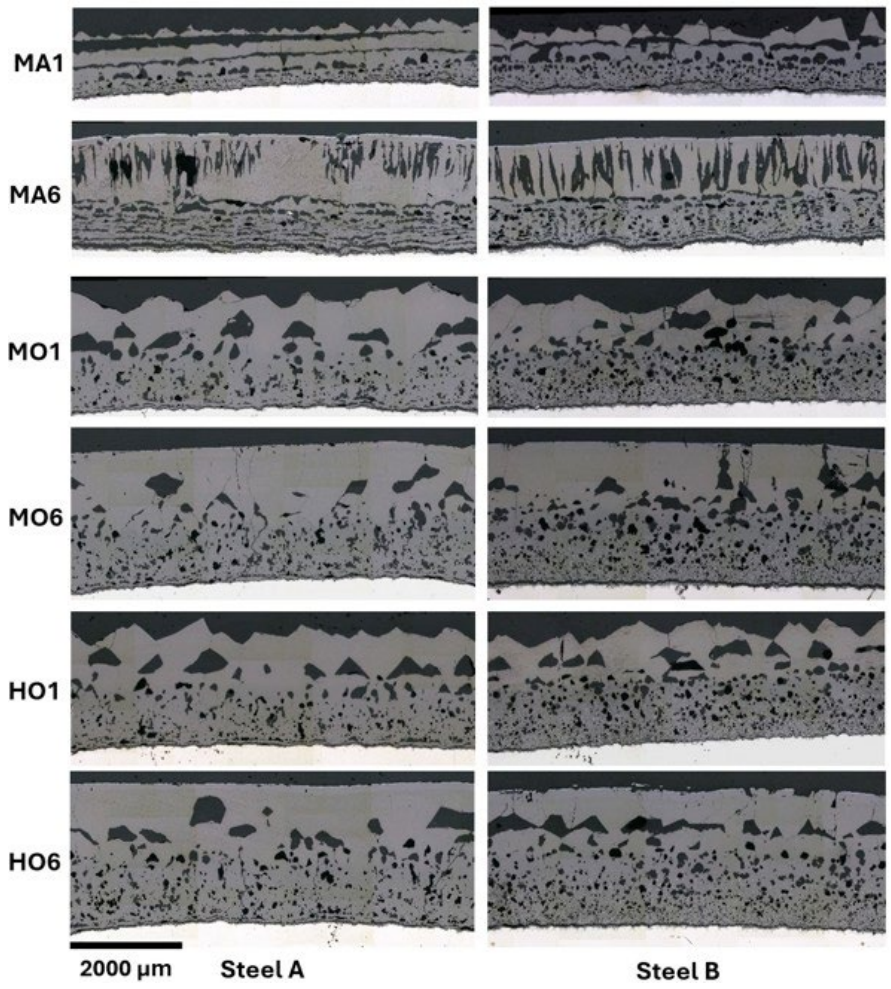

Fig.2 - Overview of oxide scale structures using different atmospheres.

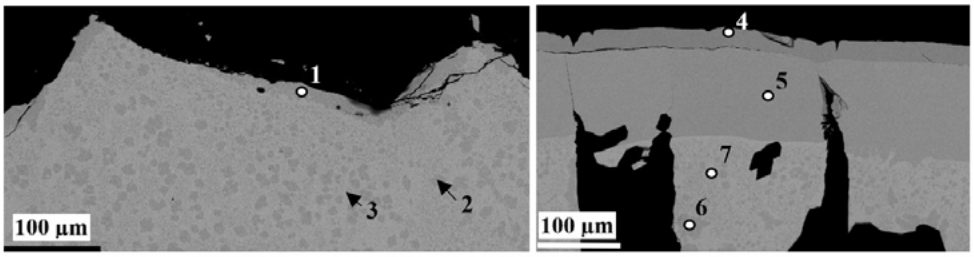

Fig.3 - Iron oxide phases at oxide-gas interface for Steel B with MA1 on the left and MA6 on the right.

Tab.4 - Elemental contents of EDS poinst (wt-%) from figure 3.

ELEMENTAL CONTENTS							
Point	1	2	3	4	5	6	7
Fe	75.4	76.5	81.0	72.0	76.8	81.3	78.0
O	24.6	23.5	19.0	28.0	23.2	18.7	22.0
Iron oxide	Fe_3O_4	Fe_3O_4	FeO	Fe_2O_3	Fe_3O_4	FeO	Fe_3O_4

Oxide-steel interfaces after heating using 6% free oxygen in gas atmospheres are presented in figure 4. A horizontal crack formed near the steel surface due to different shrinking behavior of scale and steel during cooling [19]. When looking at oxide scale below the uniform horizontal crack, methane-air method left an uneven and thicker oxide scale at the interface for Steel A, while oxide scale attached at interface is more layer-like after oxyfuel methods. For Steel B, thickness of oxide scale layer at oxide-steel interface is both thicker and more uniform using MA method compared to MO and HO methods. Pore structure can affect the cracking behavior during cooling at interface because more horizontal layered pores for air-fuel method can provide easier cracking route compared to round-shaped pores for oxyfuel methods.

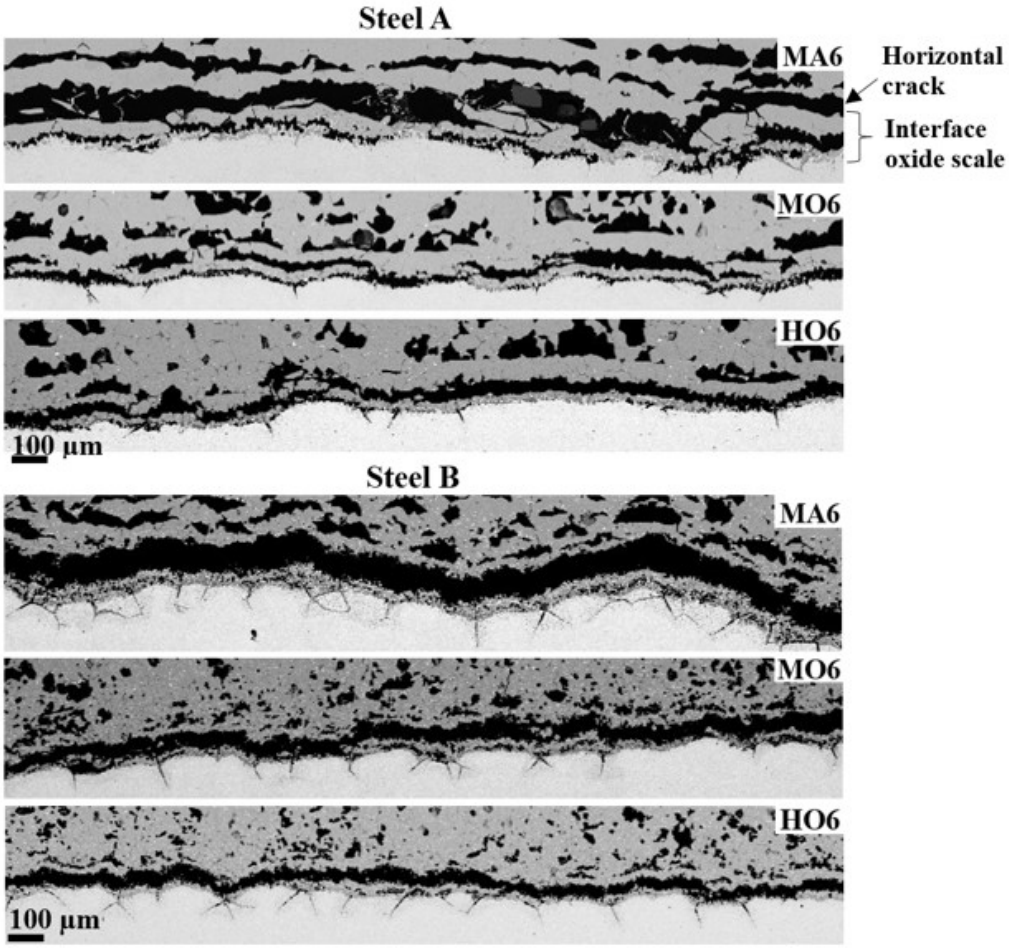

Fig.4 - Oxide-steel interface after heating with different methods.

Oxide-steel interface structures of studied steel grades are presented in figure 5, and the elemental composition of EDS points is presented in table 5. Based on EDS the lighter gray phases in oxide are wüstite (Points 1 and 4), darker gray phases are fayalite (Points 2 and 5), and white phases are metallic (Points 3 and 6). Metallic phases for Steel B are more strongly enriched with nickel compared to Steel A. Inside the steel matrix the small oxide nuclei are enriched with manganese for Steel A and manganese and chromium for Steel B as seen from EDS maps. Oxide-steel interface structure of Steel B is more entangled, and formation of pores is higher, which correlates with higher amounts of metallic phases. Oxide scale penetration inside the steel matrix into grain boundaries is more significant for Steel B, as also seen in figure 4.

La Metallurgia Italiana
International Journal of the Italian Association for Metallurgy

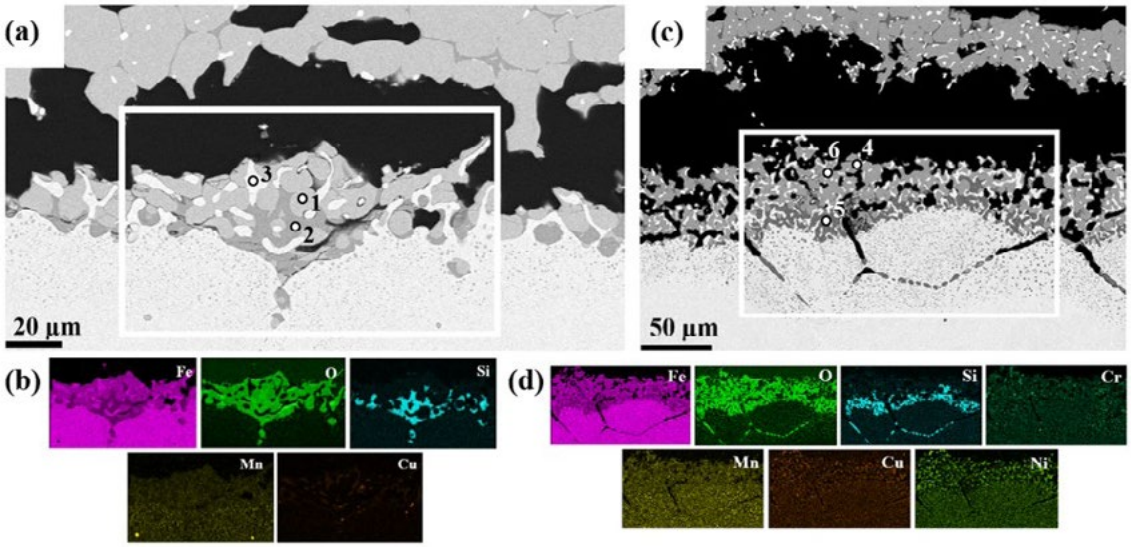

Fig.5 - Oxide-steel interface structure with EDS maps for Steel A: a) and b), and Steel B: c) and d).

Tab.5 - Elemental contents of EDS poinst (wt-%) from figure 5.

ELEMENTAL CONTENTS								
Point	Fe	O	Si	Mn	Cr	Cu	Ni	Mo
1	79.0	19.6	0.2	0.9	0.3	-	-	-
2	56.3	27.6	13.6	2.5	-	-	-	-
3	90.2	-	-	-	-	7.4	1.6	0.7
4	76.8	20.2	0.3	-	2.7	-	-	-
5	62.2	25.1	11.0	1.0	0.7	-	-	-
6	86.9	-	-	-	0.7	2.7	9.7	-

Differences in descaling efficiency by thermal shock

Steel samples oxidized with different furnace gas atmospheres and descaled by water thermal shock are presented in figure 6. The results show that descalability of Steel A was better than Steel B even though the amount of oxide formation was slightly higher for Steel A using all heating atmospheres. Transition from methane-air to hydrogen-oxygen affected the descaling efficiency of Steel A, decreasing the amount of thick outer oxide scale detached from the surface. For Steel B, the oxide scale was detached from the surface only after heating in methane-air atmosphere, although the amount of removed scale was minor for MA6. Oxide layers were not detached after heating in methane-oxygen and hydrogen-oxygen atmospheres. In addition to the heating method, free oxygen content had effect on descalability: more oxide scale was detached from the samples with lower O_2 in atmosphere. Difference between heating methods for thermal shock descaling can be based on higher H_2O and O_2 contents in atmosphere that produce thicker oxide scales with better thermal insulation [20].

Figure 6 shows that sharp-shaped surfaces from both MA1 samples were partially removed on the thick iron oxide layer when this thick layer remained on the steel surface. Similar sharp-shaped surface detaching behavior was not observed from MO1 and HO1 samples. As seen in figure 2, MA1 formed more horizontally shatter scale structures compared to other 1% O_2 containing atmospheres, indicating less adhesion inside the oxide scale.

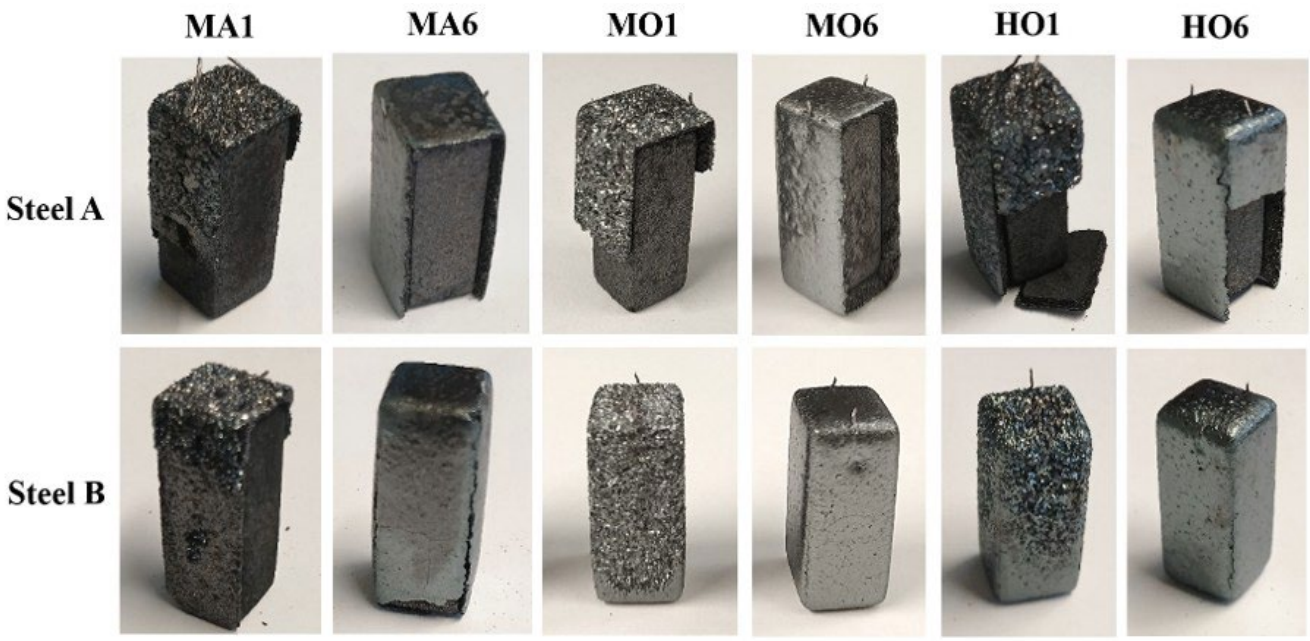

Fig.6 - Oxide scales after descaling by thermal shock.

Depending on the furnace gas atmosphere, different amounts of thick iron oxide scales are removed from the surface after descaling by thermal shock. Figure 7 shows sample sides for MA and MO methods, which still have iron oxide scale left on the surface. Oxide scale of HO methods is very similar to MO methods. Thermal shock cooling has significantly detached the outer iron oxide layer, leaving interface oxide on the steel surface. Only Steel A with MA1 method does not have a clear cooling crack in the center of the one sample side. However, all sharp-shaped outer oxide is removed on the remaining oxide layer and other three sample sides are without whole layer of outer iron oxide.

In addition to cooling cracks and sharp-shaped outer oxide removal from both steels in MA1 method by thermal shock, fast cooling causes more vertical cracking of oxide scales compared to ones without thermal shock. Furthermore, oxide scale formed using oxyfuel methods is more cohesive, while air-fuel methods have horizontal crack between more pores containing inner oxide and outer iron oxide with wide vertical voids. Similar cracking between porous inner wüstite and outer magnetite precipitates containing wüstite layer was found after air-fuel method of propane by Adolfi et al. [19], while oxyfuel method does not have crack above the porous zone. The cause of the cracks was suggested to be a lower adhesion in the oxide scale layers when cooling causes mechanical stress due to higher shrinkage of steel compared to oxide scale. Different pore structure can also be the reason for horizontal cracking. As seen in figure 4, outer line of pores inside the oxide scale of MA6 samples is almost connected horizontally to form continuous crack, while similar pore merging is not detected for oxyfuel samples.

Both vertical and horizontal cracks promote oxide scale removal in industrial descaling process, in which includes mechanical impact by water jets to remove oxide scale. Difference in pore structure and cracking between air-fuel and oxyfuel methods can be reason for observation by Adolfi et al. [19] that oxide scale formed using oxyfuel method comes off steel surface in larger pieces compared to air-fuel method.

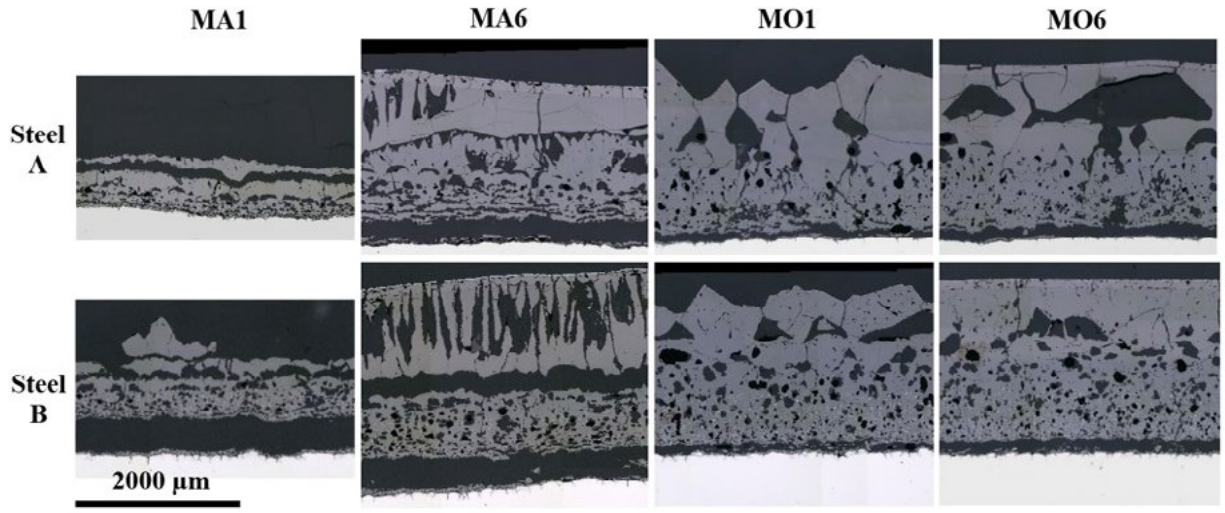

Fig.7 - Oxide scales after descaling by thermal shock.

Oxide-steel interfaces after descaling by water thermal shock are presented in figure 8. Steel A has more uneven oxide layers on the steel surface compared to more continuous layers of Steel B, indicating weaker scale adhesion. Stronger adhesion of Steel B is based on higher oxide penetration into the steel matrix and entanglement structure formation due to nickel and silicon alloying [1]. Furthermore, increase in chromium content has been reported to increase the scale adhesion [13].

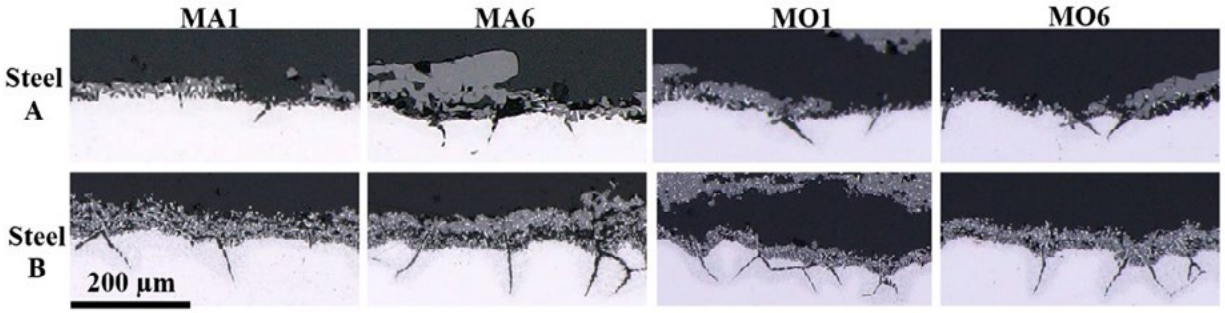

Fig.8 - Oxide-steel interface after descaling by thermal shock.

Measured thickness averages of interface oxide scale residuals on the steel surface and penetration depth averages of oxide scale pegs are presented in figure 9. Transition from methane-air to hydrogen-oxygen decreases the thickness of oxide scale at interface, indicating that heating method change can even enhance the descaling efficiency. Even if the average thickness using HO method slightly increased compared to MO methods for Steel A, the thickness of the residual scale is still lower than the methane-air method (MA6). Higher unevenness and variation in measured average thickness of residual oxide scales after MA methods can be the result of different pore structures between air-fuel and oxyfuel methods. Similar unevenness of internal oxide scale after MA methods was observed in samples without thermal shock descaling (figure 3).

Average penetration depths of oxide scale pegs into the steel matrix are about 30 µm for Steel A and about 55 µm for Steel B as seen in figure 9b. Variations of depths is minor and therefore no significant effect of heating method on oxide scale peg depths can be observed. In consideration of interface oxide thickness and depths of oxide pegs, there is not a noticeable decrease in descaling efficiency in transition of heating methods from methane-air to hydrogen-oxygen, when industrial descaling with mechanical impact can also remove thick outer iron oxide scale layer from the steel surface.

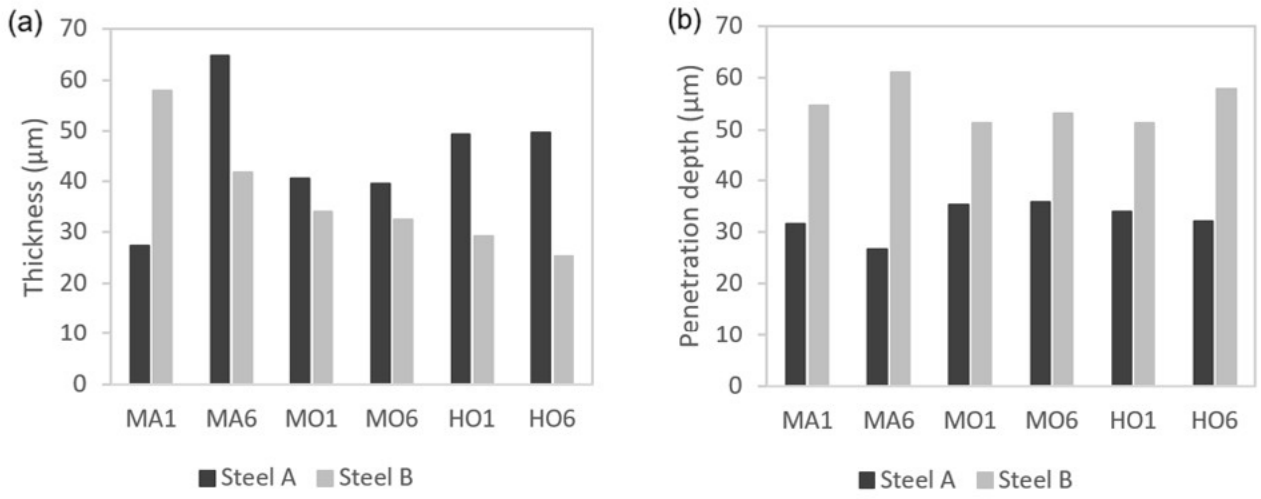

Fig.9 - Heating atmosphere differences for oxide-steel interface after thermal shock: a) oxide scale thickness at interface and b) penetration depth of oxide scale.

CONCLUSIONS

The influence of simulated furnace atmosphere between current methane-air, methane-oxygen, and hydrogen-oxygen heating methods on thermal shock descaling efficiency was investigated for low-carbon steels. Oxide scale formation increased by increasing amount of water vapor and oxygen in the heating atmosphere, and the descaling efficiency by thermal shock decreases by changing heating method from methane-air to hydrogen-oxygen. The higher amount of nickel and chromium containing Steel B oxidized less in all studied heating methods, but its descaling efficiency by water thermal shock was weaker compared to Steel A. Lower free oxygen content (1%) removed oxide from a wider sample surface area, but regardless of free oxygen content, oxyfuel based oxide scales for Steel B remained unchanged after descaling. Thickness of residual oxide scale at oxide-steel interface decreased between methane-air and hydrogen-oxygen methods for both steel grades, and oxide scale penetration depths were similar between methods. Thus, the change of the heating methods has not been found to have a decreasing effect on oxide-steel interface quality after thermal shock descaling.

ACKNOWLEDGEMENTS

This research was part of the Strategic Research Council within the Research Council of Finland project JustH-2Transit (decision 358422). The authors wish to thank Ovako Imatra Oy Ab for supplying materials, and the Centre for Material Analysis, University of Oulu, Finland, for supporting this work.

REFERENCES

[1] Melfo W., Bolt H., Rijnders M., Staalman D., Castro C.B., Crowther D., Jana B., Experimental study on primary scale formation and descalability on steels containing Ni and Ni+ Si. ISIJ int. 2013;53:866–873.

[2] Ramírez-Cuellar J., Guerrero-Mata M.P., Leduc L.A., Colás R., Modelling the oxide growth during hot rolling of low carbon steel in a compact mill. Conference Proceedings - International Conference on Thermomechanical Processing: Mechanics, Microstructure & Control. 2003. p. 418–422.

[3] Haapakangas J., Riikonen S., Airaksinen S., Heikkinen E.P., Fabritius T., Oxide scale formation on low-carbon steels in future reheating conditions. Metals. 2024;14:189.

[4] Ojiako T.P., Buchely M.F., Lekakh S., O'Malley R.J., Osei R., Tayebali T., Parametric analysis of water jet descaling efficiency of reheated continuously cast thin slab. Steel Res. Int. 2026;97:758–772.

[5] Bendig L., Raudenský M., Horský J., Descaling with high pressure nozzles. Conference Proceed-ings - the 17th European Conference on Liquid Atomization and Spray Systems. 2001. pp. 742-747.
[6] Horsky J., Raudensky M., Vavrecka L., Experimental study of hydraulic descaling. Conference Pro-ceedings - 5th International Conference on Heat Transfer, Fluid Mechanics and Thermodynamics, 2007 Jul 1-4; South Africa; 2007.
[7] Basabe V.V., Szpunar J.A., Effect of O2 in heating atmosphere on hydraulic descaling in hot rolling of low carbon steel. ISIJ int. 2008;48:467-474.
[8] Luzzo I., Cirilli F., Jochler G., Gambato A., Longhi J., Rampinini G., Feasibility study for the utiliza-tion of natural gas and hydrogen blends on industrial furnaces. Mater Tech. 2021;109:306.
[9] Abuluwefa H.T., Guthrie R.I.L., Ajersch F., Oxidation of low carbon steel in multicomponent gases: Part I. Reaction mechanisms during isothermal oxidation. Metall Mater Trans A. 1997;28:1633–1641.
[10] Haapakangas J., Airaksinen S., Heikkinen E.P., Fabritius T., Oxidation of Carbon Steels in Novel Reheating Conditions: Changes to Oxidation Kinetics. Metall Mater Trans B, 2025;56:3762–3773.
[11] Rahmel A., Tobolski J., Einfluss von wasserdampf und kohlendioxyd auf die oxydation von eisen in sauerstoff bei hohen temperaturen. Corros. Sci, 1965;5:333–346.
[12] Vedaei-Sabegh A., Morin J.B., Jahazi M., Influence of Nickel on High-Temperature Oxidation and Characteristics of Oxide Layers in Two High-Strength Steels. Steel Res Int. 2020;91:1900536.
[13] Takeda M., Kushida H., Onishi T., Toyama M., Koizumi F., Fujimoto S., Influence of oxidation tem-perature and Cr content on the adhesion and microstructure of scale on low Cr steels. Oxid. Met. 2010;73:1–13.
[14] Park S.-Y., Xiao X., Kim M.-J., Lee G.-T., Hwang D.-H., Woo Y.-H., Lee D.-B., Oxidation of Fe-(5.3-29.8)% Mn-(1.1-1.9)% Al-0.45% C Alloys at 550-650℃. Corros. Sci. Technol. 2022;21:53–61.
[15] Aghaeian S., Sloof W.G., Mol J.M.C., Böttger A.J., Initial high-temperature oxidation behavior of Fe–Mn binaries in air: the kinetics and mechanism of oxidation. Oxid. Met. 2022;98:217–237.
[16] Airaksinen S., Haapakangas J., Gyakwaa F., Heikkinen E.P., Fabritius T., Utilization of hydrogen fuel in reheating furnace and its effect on oxide scale formation of low-carbon steels. Int. J. Hydrog. Energy. 2025;140:1212–1220.
[17] Haapakangas J., Airaksinen S., Heikkinen E.P., Fabritius T., Oxide Scale Morphology of Carbon Steels Under Novel Reheating Conditions. Steel Res Int. 2026:1–13.
[18] Oleksak R.P., Kapoor M., Perea D.E., Holcomb G.R., Doğan Ö.N., The role of metal vacancies during high-temperature oxidation of alloys. npj Mater. Degrad. 2018;2:25.
[19] Adolfi J., Ekman T., von Schéele J., Blasiak W., Scale formation and surface quality of carbon steel at oxyfuel heating. Steel Rolling. Paris; 2006.
[20] Sherwood W., Shatynski S.R., The effect of temperature on oxide scale adherence during descaling operations. Surf. technol. 1984;21:39–51.

TORNA ALL'INDICE >